Published in final edited form as:
Cell. 2009 November 25; 139(5): 891–906. doi:10.1016/j.cell.2009.10.027.

Matrix Crosslinking Forces Tumor Progression by Enhancing Integrin signaling

Kandice R. Levental[1,*], **Hongmei Yu**[2,*], **Laura Kass**[2], **Johnathon N. Lakins**[2], **Mikala Egeblad**[**,4], **Janine T. Erler**[3], **Sheri F.T. Fong**[5], **Katalin Csiszar**[5], **Amato Giaccia**[3], **Wolfgang Weninger**[6], **Mitsuo Yamauchi**[7], **David L. Gasser**[8], and **Valerie M. Weaver**[1,2,4,9,10]

[1] Department of Bioengineering and Institute for Medicine and Engineering, University of Pennsylvania, Philadelphia, PA 19104

[2] Center for Bioengineering and Tissue Regeneration, Department of Surgery, University of California at San Francisco, San Francisco, CA 94143

[3] Department of Radiation Oncology, Stanford University School of Medicine, Stanford, CA 94305

[4] Department of Anatomy, University of California at San Francisco, San Francisco, CA94143

[5] Cardiovascular Research Center, John A. Burns School of Medicine, University of Hawaii at Manoa, Honolulu, HI 96822

[6] Immunology Program, Wistar Institute, Philadelphia, PA 19104

[7] Dental Research Center, University of North Carolina, Chapel Hill, NC 27599

[8] Department of Genetics, University of Pennsylvania, Philadelphia, PA 19104

[9] Department of Bioengineering and Therapeutic Sciences, Eli and Edythe Broad Center of Regeneration Medicine and Stem Cell Research at UCSF and Helen Diller Comprehensive Cancer Center at UCSF, University of California at San Francisco, San Francisco, CA 94143

Summary

Tumors are characterized by extracellular matrix (ECM) remodeling and stiffening. The importance of ECM remodeling to cancer is appreciated; the relevance of stiffening is less clear. We found that breast tumorigenesis is accompanied by collagen crosslinking, ECM stiffening and increased focal adhesions. Inducing collagen crosslinking stiffened the ECM, promoted focal adhesions, enhanced PI3 Kinase (PI3K) activity, and induced the invasion of an oncogene-initiated epithelium. Inhibiting integrin signaling repressed the invasion of a premalignant epithelium into a stiffened, crosslinked ECM, and forced integrin clustering promoted focal adhesions, enhanced PI3K signaling and induced the invasion of a premalignant epithelium. Consistently, reducing lysyl oxidase-mediated collagen crosslinking prevented MMTV-Neu-induced fibrosis, decreased focal adhesions and PI3K activity, impeded malignancy and lowered tumor incidence. These data show how collagen crosslinking can modulate tissue fibrosis and stiffness to force focal adhesions, growth factor signaling and breast malignancy.

10 Address all correspondence to: Valerie M. Weaver Ph.D., Associate Professor and Director, Center for Bioengineering and Tissue Regeneration, Department of Surgery, University of California, San Francisco, 513 Parnassus Avenue, S1364, Box 0456, San Francisco, CA 94143-0456, Telephone: 415 476-3826, weaverv@surgery.ucsf.edu.
*Both authors contributed equally to the work
**Current Address: Cold Spring Harbor Laboratory, Cold Spring Harbor, NY 11724

Introduction

The tumor stroma is characterized by extracellular matrix (ECM) remodeling and stiffening and tissue stiffness has been exploited to detect cancer (Butcher et al., 2009; Sinkus et al., 2000). ECM stiffness enhances cell growth and survival and promotes migration (Lo et al., 2000), and ECM rigidity disrupts tissue morphogenesis by increasing cell tension (Paszek et al., 2005). Reducing cell tension repressed the malignant behavior of mammary epithelial cells (MECs) and normalized the behavior of breast cancer cells in culture (Paszek et al., 2005). What drives ECM stiffening in tumors and whether ECM tension could drive tumor progression has yet to be determined.

Collagen is the most abundant ECM scaffolding protein in the stroma and contributes significantly to the tensile strength of tissue (Kolacna et al., 2007). Collagen metabolism is deregulated in cancer, where increased collagen expression, elevated deposition, altered organization, and enhanced matrix metalloproteinase (MMP) activity and collagen turnover have been implicated in tumor progression (Jodele et al., 2006). MMP-mediated collagen remodeling can create space for cells to migrate, produce substrate cleavage fragments with independent biological activity, modify adhesion to regulate tissue architecture, and activate, deactivate, or alter the activity of signaling molecules (Page-McCaw et al., 2007). Although high levels of MMPs correlate with poor prognosis in cancer patients (Tetu et al., 2006), and modulating MMP activity changes tumor phenotype (Zhang et al., 2008), MMP inhibitors failed clinically (Coussens et al., 2002), indicating other ECM remodeling parameters regulate malignancy.

Type I collagen is considered a structural barrier against tumor invasion, paradoxically, increased expression of collagen is associated with elevated incidence of metastasis (Ramaswamy et al., 2003). Indeed, mammographic density, which is characterized by higher collagen I, increases breast cancer risk (Martin and Boyd, 2008). Importantly, collagen crosslinking accompanies tissue fibrosis (van der Slot et al., 2005) and fibrosis increases risk to malignancy (Colpaert et al., 2003). Lysyl oxidase (LOX), a copper-dependent amine oxidase (Kagan and Li 2003) which initiates the process of covalent intra- and intermolecular crosslinking of collagen by oxidatively deaminating specific lysine and hydroxylysine residues located in the telopeptide domains (Yamauchi and Shiiba, 2008), is frequently elevated in tumors (Erler et al., 2009). Active LOX stiffens tissues and can compromise their function (Pfeiffer et al., 2005) and reducing LOX activity tempers tissue stiffness and prevents fibrosis (Georges et al., 2007). Nevertheless, the relationship between collagen crosslinking, tissue fibrosis and tension and cancer has yet to be assessed.

Integrins transduce cues from the ECM by assembling adhesion plaque complexes that initiate biochemical signaling and stimulate cytoskeletal remodeling to regulate cell behavior (Miranti and Brugge, 2002). Force increases integrin expression, activity and focal adhesions (Paszek et al., 2005; Sawada et al., 2006). Human breast tumors are often fibrotic and stiff, and breast cancer cells that exhibit high tension have elevated integrins and focal adhesions and increased integrin signaling (Madan et al., 2006; Mitra and Schlaepfer, 2006). Thus ECM stiffness could regulate malignancy by enhancing integrin-dependent mechanotransduction. Consistently, breast malignancy can be inhibited by genetically ablating integrin expression (White et al., 2004), and breast cancer cell behavior can be repressed by inhibiting integrin activity or reducing cell tension (Paszek et al., 2005). Likewise, knocking down the expression or inhibiting the function of focal adhesion kinase (FAK) or ^{p130}Cas, two integrin adhesion proteins, impedes breast tumor progression (Cabodi et al., 2006; Lahlou et al., 2007). Here, we asked if collagen crosslinking could stiffen the ECM and induce fibrosis to promote breast

malignancy by altering integrins and whether inhibiting collagen crosslinking could prevent fibrosis and impede breast tumorigenesis by reducing integrin signaling.

Results

ECM stiffening and collagen crosslinking accompany breast tumor progression

The HER2 gene is a member of the epidermal growth factor receptor (EGFR) family that is amplified in 20-25% of human breast cancers. The murine equivalent of HER2 is the wild type Neu transgene which under the MMTV promoter (MMTV–Neu) develops breast tumors with a long latency (Kim and Muller, 1999). Using the MMTV-Neu model we studied the relationship between tissue fibrosis, stiffness and cancer. Unconfined compression and rheological testing showed an incremental stiffening of the mammary gland as it transitioned from normal to premalignant to invasive cancer (Fig 1A, B & C top) and demonstrated that the stromal tissue adjacent to the invading epithelium was also substantially stiffer than normal. Total levels (Supp Fig 1) and amount of fibrillar collagen increased markedly (Fig 1C & D) and second harmonics generation (SHG) imaging revealed the progressive linearization of the collagen adjacent to the developing epithelial lesions (Fig 1E & F).

We next explored if collagen crosslinking could account for the dramatic ECM remodeling and stiffening. We noted an increase in the levels of the major reducible bifunctional collagen crosslinks, dehydrodihydroxylysinonorleucine (DHLNL) and hydroxylysinonorleucine (HLNL), in the breast tumors, reflecting elevated crosslinked collagen (Fig 1G). We further detected increased amounts of the amine oxidase crosslinking enzyme, LOX in the stromal cells of the premalignant Min foci and invasive tumors, and in the invading transformed epithelium (Fig 1H). These data establish an association between collagen crosslinking, LOX expression, ECM stiffness and tissue fibrosis in Neu-induced breast tumorigenesis.

LOX-mediated collagen crosslinking and tissue stiffening promote focal adhesions and tumor progression *in vivo*

We next asked if LOX-mediated collagen crosslinking could stiffen the breast and promote invasion of a premalignant lesion. We used Ha-ras human MCF10AT MECs which upon injection into mice develop into premalignant tissues (Hu et al., 2008). We conditioned inguinal mammary fat pads of NOD/SCID mice, surgically-cleared of their epithelium, with control fibroblasts or those expressing elevated LOX (Fig 2A; Supp Fig 2 & 3). Rheological measurement revealed that the mammary glands conditioned with LOX expressing fibroblasts were stiffer (Fig 2B), picrosirius red staining showed they had more fibrillar collagen (Fig 2C & D), and SHG imaging revealed they had more linearized collagen (Fig 2C & E). Consistent with ECM stiffening, resident fibroblasts in the epithelial-cleared LOX-treated glands showed more FAK^{pY397} and ^{p130}Cas immunostaining, indicative of increased focal adhesions and mechanosignaling in the stromal cells (Fig 2C; bottom).

LOX pre-conditioning and stiffening of the mammary gland promoted the growth and invasion of Ha-ras premalignant mammary organoids injected into these tissues as revealed by a significant increase in lesion size and tumors that lacked margins (Figs 2F, G & H). MECs in the LOX pre-conditioned glands also had more focal adhesions, as revealed by elevated FAK^{pY397} (Fig 2H) and ^{p130}Cas (not shown). To rule out any direct effect of LOX activity on MEC behavior, we also treated a cohort of animals in parallel (i.e. at time of MEC injection) with β–aminopropionitrile (BAPN), a natural and irreversible inhibitor of lysyl oxidase activity (Kagan and Li, 2003). Because BAPN treatment had no effect on tumor growth, invasion and focal adhesions (Supp Fig 4, 5, & 6) we concluded that it was LOX pre-conditioning of the stroma and gland stiffness that promoted mammary tumor progression, and not any direct effect of LOX on the mammary epithelium. These findings demonstrate how ECM crosslinking and

stiffening can induce focal adhesions and promote the growth and invasion of an oncogene-initiated mammary epithelium *in vivo*.

Inhibiting LOX-mediated collagen crosslinking decreases fibrosis and reduces focal adhesions to inhibit breast tumor progression *in vivo*

We next asked if reducing LOX-dependent collagen crosslinking could temper tissue fibrosis and decrease focal adhesions, and whether this would inhibit breast tumor progression. We inhibited LOX activity using the cell soluble BAPN (Lucero and Kagan, 2006) or a LOX-specific function-blocking polyclonal which only inhibits extracellular LOX activity (Erler et al., 2006) and assayed collagen crosslinking, tissue fibrosis, focal adhesions and breast tumor development.

Inhibition of LOX activity was initiated in five month old parous animals, when LOX levels were already increased in the stromal cells but were non-detectable in the mammary epithelium (Fig 1H). Treatment was continued for one month after which the animals were allowed to recover for another month and then sacrificed (Fig 3A). At time of sacrifice, the non-treated MMTV-Neu mice had high levels of active LOX in the serum whereas BAPN or LOX inhibitory polyclonal-treated animals had reduced levels (Fig 3B). Mice with reduced LOX activity showed significant decreases in LOX-mediated collagen crosslinks, both reducible (DHLNL and HLNL) and nonreducible (pyridinoline) (Fig 3C & D), and the collagen fibrils adjacent to the epithelial lesions were less linear (Fig 3E & F). Consistent with the possibility that inhibiting collagen crosslinking prevented tissue fibrosis, LOX inhibition reduced fibrillar collagen (Fig 3G & H) and had reduced focal adhesions, as indicated by negligible FAK^{pY397} (Fig 3I).

Inhibiting LOX activity also increased tumor latency (Fig 4A) and decreased tumor incidence (Fig 4B), despite ErbB2 activity (Fig 4C). Moreover, the palpable lesions formed in the LOX-inhibited animals were smaller (Fig 4D) and less proliferative (Fig 4E). LOX inhibited mammary glands also stained positively for cytokeratin 14 along the basal periphery of the ducts, implying retention of their myoepithelium (Fig 4H & I). H&E sections revealed that a significantly greater proportion of the lesions in the LOX-inhibited animals were hyperplastic or premalignant (hyperplastic alveolar nodules, HAN, or mammary intraepithelial neoplasia, MIN) and the tumors that did develop were mostly low grade as opposed to the high grade carcinomas typically observed in the untreated Neu mice (Fig 4G & F). These results show how inhibiting LOX activity reduces collagen crosslinking, tempers tissue fibrosis, decreases focal adhesions, and impedes tumor progression to reduce breast tumor incidence.

Collagen crosslinking and ECM stiffening promote focal adhesions and drive invasion of oncogenically-initiated mammary tissues in culture

We next assessed the effect of non-specifically inducing collagen crosslinking and stiffening on MEC invasion in the absence of fibroblasts, immune cells and other stromal and systemic cellular and soluble factors (Fig 5A experimental schemata). We explored the effect of nonspecific collagen crosslinking and stiffening on tumor invasion by adding nonmetabolizable L-ribose to the media of nonmalignant, MCF10A acini embedded in a 3D soft collagen I/reconstituted basement membrane gel (Col/rBM gel).

To determine whether MEC invasion required oncogenic signaling we utilized MCF10As expressing an ErbB2 chimera (ErbB2.chim; called HER-2; the human homologue of Neu) consisting of the extracellular and transmembrane domains of low-affinity nerve growth factor receptor (p75NGFR), and the cytoplasmic kinase domain of ErbB2 linked to the synthetic ligand-binding domain from the FK506-binding protein (FKBP). In these MECs addition of the synthetic bivalent FKBP ligand, AP1510, drives homodimerization of ErbB2, activation

of the kinase domain and initiation of ErbB2 signaling (Muthuswamy et al., 2001). Chimeric ErbB2 signaling drives proliferation and luminal filling but fails to induce MEC invasion in rBM (Fig 5E). To study effects of homo- (ErbB2/ErbB2) and heterodimer (ErbB1/ErbB2) formation we also engineered MECs in which the wild type ErbB2 could be overexpressed through addition of doxycycline (ErbB2.TetOn; Supp Fig 7 & 8).

In the absence of ErbB2 activity MECs in collagen/rBM gels assembled acini, as illustrated by basally-oriented β4 integrin and cell-cell localized beta catenin (Fig 5E). Glycation-mediated crosslinking stiffened the collagen (Fig 5B), increased colony size (Fig 5C), and disrupted tissue organization, as revealed by diffusely localized beta catenin and the appearance of random cells within the lumens (Fig 5E). MECs within the ribose crosslinked collagen gels also had elevated levels and co-localized β1 integrin and FAK^{pY397}, indicative of tension-induced focal adhesions (Fig 5D). Nevertheless, in the absence of ErbB2 activity, ECM stiffening did not drive MEC invasion (Fig 5E & F).

Addition of either AP1510 (1μM) or doxycycline (0.2μg/mL) to the mammary acini, induced and activated (ErbB2.TetOn) or directly activated ErbB2 (ErbB2.chim) (Supp Fig 9), promoted cell growth (not shown), drove luminal filling, and destabilized cell-cell junctions, as revealed by diffusely localized beta catenin (Fig 5E). Sustained ErbB2 activation did not drive MEC invasion, as indicated by colony integrity and the retention of basally-localized β4 integrin (Muthuswamy et al., 2001); Fig 5E & F). Yet, when ErbB2 was activated in colonies in the crosslinked, stiffened gels, colony architecture disintegrated, as revealed by the absence of detectable beta catenin and disorganized β4 integrin staining, and MECs invaded into the gels (Fig 5E & F). SHG imaging revealed that ErbB2 activation and ECM stiffening was accompanied by the appearance of prominent collagen bundles surrounding the colonies, and showed that single MECs invaded on fibrils that extended perpendicularly into the crosslinked, stiffened gels following ErbB2 activation (Fig 5E; Supp Fig 9). These findings show how collagen crosslinking and ECM stiffening, per se, cooperate with oncogenes such as ErbB2 to promote the invasive behavior of a mammary epithelium.

Interestingly, confocal imaging revealed elevated ^{p130}Cas and FAK^{pY397} staining that co-localized with β1 integrin (colocalization analysis of FAK^{pY397} and β1 integrin; Pearson's r = 0.78; ^{p130}Cas and β1 integrin, Pearson's r = 0.89) in the stiffer breast tissue of the Neu mice (Fig 6A; see insert) and reduced levels of FAK^{pY397} following LOX inhibition (Fig 3H). Moreover, inhibiting β1 integrin activity, using the function blocking antibody AIIB2, or reducing integrin signaling by expressing an inducible FRNK (FRNK.TetOn; Supp Fig 10) prevented the force-mediated invasion of the ErbB2 activated mammary organoids (Fig 5G & H). These findings show how ECM crosslinking and stiffness cooperate with an oncogene to promote breast cell invasion and implicate integrin signaling in force-dependent tumor progression.

Integrin clustering promotes focal adhesions to drive invasion of a Ha-ras mammary epithelium *in vitro* and *in vivo*

To determine if integrin signaling would be sufficient to induce breast tumor invasion we expressed a series of integrin constructs in nonmalignant MCF10A and Ha-ras premalignant MCF10AT MECs and assayed for invasive behavior in rBM and *in vivo* (Fig 6B).

Expression of the V737N integrin, which recapitulates tension-dependent integrin clustering, promoted focal adhesions, indicated by elevated FAK^{pY397} (Fig 6C) and disrupted the integrity of mammary colonies in rBM, revealed by luminal filling and altered β4 integrin localization (Fig 6C; top). In contrast, neither expression of a wild type (Fig 6C) nor a constitutively active β1 integrin (not shown; (Paszek et al., 2005)) induced focal adhesions and disrupted mammary tissue architecture. Moreover, while the V737N β1 integrin mutant failed to promote invasion

of the MCF10A MECs (Fig 6C), the V737N integrin induced the invasion of the Ha-ras premalignant MCF10AT colonies in rBM (Fig 6D & E). Upon injection into nude mice the V737N integrin not only promoted focal adhesions, and increased lesion size (Fig 6F), but also induced the invasive behavior of the Ha-ras MCF10AT organoids, as revealed by the loss of epithelial lesion margins and increased FAK^{pY397}(see arrows in Fig 6G). These findings implicate tension-dependent integrin clustering and focal adhesions in breast tumor invasion. However, because integrin clustering could only promote invasion in Ha-ras premalignant MECs, they also illustrate how integrin-mediated mechanotransduction cooperates with oncogenic signaling to drive malignancy.

Collagen crosslinking and tissue stiffness promote integrin clustering and enhance PI3K signaling to regulate invasion of a premalignant mammary epithelium *in vitro* and tumor progression *in vivo*

Integrins active PI3K, and PI3K promotes invasion in culture and tumor progression *in vivo* (Webster et al., 1998). Therefore, we explored the relationship between focal adhesions and PI3K signaling in tension-dependent breast tumor invasion. We found Akt signaling, an established target of PI3K, to be elevated in the premalignant and malignant, rigid mammary tissue (Fig 7A) and in the mammary colonies in the ribose-stiffened collagen gels (Fig 7B).

We examined the effect of ECM rigidity on PI3K activity in MECs plated on rBM-functionalized polyacrylamide gels (rBM PA gel) with elastic moduli of 140-400 (soft) and ≥5000-10,000 (stiff) Pascals. These two extremes represent the ECM stiffness of healthy versus transformed breast tissue. Although substrate stiffness did not increase the levels of Akt^{pS473} in unstimulated MECs, ECM stiffness potentiated the magnitude of EGF-activated Akt^{pS473} (Fig 7C) and increased ErbB2-activated Akt^{pS473} (Fig 7D). MECs on soft gels that expressed the β1 integrin cluster mutant, but not the wild-type β1 integrin, also showed a significant increase in Akt^{pS473} activity following EGF stimulation. These results suggest integrin mechanotransduction potentiates growth factor dependent PI3 kinase signaling (Fig 7E; Fig 6B & C).

Pharmacological inhibition of PI3K activity with LY294002 restored the colony architecture of ErbB2-activated MECs in ribose crosslinked collagen gels towards that of a non-invasive, polarized, cohesive colony (Fig 7F & G). Inhibiting PI3K activity reduced colony size, and immunostaining revealed that colonies treated with LY294002 retained β catenin at cell-cell junctions and had basally-localized β4 integrin (Fig 7F). The epithelium from the LOX-inhibited Neu mice also had lower PI3K signaling, as revealed by fainter active Akt/PI3K Substrate staining (Fig 7H). These data are consistent with a role for integrin mechanotransduction in PI3K-mediated breast tumor invasion. The findings suggest that ECM stiffness, as induced by elevated collagen crosslinking could promote breast malignancy by enhancing integrin-GFR crosstalk (Fig 7I; (Miranti and Brugge, 2002)).

Discussion

Our findings identify collagen crosslinking as a critical regulator of desmoplasia and imply that the level and nature of ECM crosslinks in a tissue could impact cancer risk and alter tumor behavior. The observations are consistent with links between ECM crosslinking and tissue stiffening in tissue fibrosis and could explain the increased risk to malignancy associated with these conditions (Colpaert et al., 2003). They might also explain why women with mammographically dense breasts have an increased relative risk of developing cancer (Martin and Boyd, 2008). Because aged tissues are stiffer and contain high levels of aberrant collagen crosslinks, the data offer a new paradigm for understanding why tumor incidence increases so dramatically with aging (Szauter et al., 2005).

Tissue fibrosis influences tumor progression by regulating soluble factors that induce inflammation and angiogenesis and stimulate cell growth and invasion (Bierie et al., 2009; Coussens et al., 1999). We showed that modifying the state of collagen crosslinking and ECM stiffness, two physical parameters of the tissue microenvironment, modulated the invasive behavior of an oncogene pre transformed mammary epithelium, even in the absence of cellular and soluble tissue and systemic factors. The findings imply that tissue fibrosis could regulate cancer behavior by influencing the biophysical properties of the microenvironment to alter force at the cell and/or tissue level. Importantly, we noted that focal adhesions were elevated in the stiffened breast tumors and organoid cultures, that forcing focal adhesions promoted MEC invasion and that inhibiting focal adhesion signaling or tempering tissue stiffening reduced focal adhesions and tumor invasion. These observations are consistent with the notion that force regulates the invasive behavior of tumors by modulating integrin activity and focal adhesion assembly and signaling (Paszek et al., 2005). The findings thereby provide an explanation for why ^{pY}FAK and ^{p130}Cas are so often increased in breast tumors (Cabodi et al., 2006; Madan et al., 2006), even when integrin expression is frequently decreased (Koukoulis et al., 1993; Zutter et al., 1998). Indeed, the observations suggest that enhanced integrin signaling rather than just an increase in integrin expression is more critical for tumor progression.

Our data show how modulating the activity of one class of ECM crosslinking enzymes, the LOXs, can directly modify tumor progression by regulating collagen crosslinking and stiffness. The results are consistent with data indicating that LOX enzymes are elevated in many cancers (Erler and Weaver, 2009) and that LOX is induced by hypoxia inducible factor (HIF-1) and TGFβ; two key regulators of tumor behavior (Postovit et al., 2008). Indeed, cellular LOX promotes breast cell migration and invasion and enhances tumor proliferation and survival (Kirschmann et al., 2002). Hypoxia-induced LOX modulates tumor metastasis by regulating integrin function (Erler and Giaccia, 2006), by facilitating tumor extravasation (Bondareva et al., 2009) or by conditioning the metastatic niche (Erler et al., 2009). Our work indicates that LOX can promote tumor progression and MEC invasion by increasing fibrillar collagen and ECM stiffness. These observations are consistent with the major function of LOX in tissues as a key enzyme for collagen and elastin crosslinking that enhances tensile strength (Szauter et al., 2005). Consistently, by inhibiting LOX activity early, when levels were high in the stroma we prevented ECM remodeling and stiffening and reduced tumor progression in the MMTV-Neu mice. Because a LOX-specific inhibitory polyclonal that cannot inhibit intracellular LOX also prevented fibrosis and tumor progression our results suggest that LOX-mediated collagen crosslinking likely regulates breast tumor progression by modifying the tumor microenvironment rather than by directly changing cell behavior.

We observed that LOX inhibition reduced focal adhesions and PI3K signaling indicating that LOX modulates breast tumor progression by stiffening the ECM to drive focal adhesions assembly and enhance GFR-dependent PI3K signaling. Consistently, we showed that ribose-mediated collagen crosslinking, which induces nonspecific collagen glycation, also stiffened the ECM and enhanced focal adhesions and PI3K signaling to promote ErbB2-dependent breast tumor invasion. We noted that MEC invasion could be abrogated by inhibiting integrin and FAK activity, thereby illustrating the importance of ECM crosslinking and stiffness in tumor progression. This idea is consistent with our recent findings that LOX conditioning of the lung ECM promotes breast tumor metastasis (Erler et al., 2009), and data showing that fibrotic breast tumors have the poorest prognosis and highest rate of recurrence (Hasebe et al., 1997). Indeed, our findings underscore the notion that ECM crosslinking and stiffness, per se, is a key regulator of tumor progression. They imply that other ECM crosslinkers/modulators implicated in tissue fibrosis such as tissue transglutaminase, lysyl hydroxylase or some of the proteoglycans or even non-specific metabolic glycation end products (AGEs) might also similarly promote malignancy.

LOX has been proposed to be a tumor suppressor (Payne et al., 2007) possibly by directly inhibiting ECM adhesions and integrin signaling (Zhao et al., 2008). LOX-mediated ECM stiffening could also impede cell invasion in the absence of MMP activity (Zaman et al., 2006) reminiscent of highly crosslinked, stiff fibrotic tissues and scars that often never progress to malignancy. We noted that neither ECM stiffness nor forced integrin clustering induced mammary tissue invasion in the absence of oncogenic signaling. This suggests that other factors that modulate integrins and/or ECM remodeling or cellular tension likely cooperate with ECM crosslinking and force to promote tumor invasion (Katz et al., 2007; Wolf et al., 2007). Instead, ECM stiffness appears to operate as a signaling rheostat potentiating oncogenic cues to promote tumor invasion.

Cancer progression is accompanied by MMP-dependent ECM remodeling. Multiple MMPs are over expressed in the tumor stroma, and some MMPs are up regulated in transformed epithelia (Jodele et al., 2006; Page-McCaw et al., 2007). Elevated expression of specific MMPs induced desmoplasia and malignant transformation (Sternlicht et al., 1999) and genetic ablation of MMPs or pharmaceutical inhibition of MMP activity reduced breast metastasis (Martin et al., 2008). These data argue that MMPs are critical for malignancy. Nevertheless, clinical trials with MMPs failed, suggesting the role of MMPs in cancer is more complicated (Coussens et al., 2002). Indeed, MMPs collaborate with crosslinking enzymes such as LOX to facilitate collagen maturation, and MMPs and LOX regulate the expression and activity of soluble factors such as transforming growth factor beta that regulate tumor cell behavior (TGFβ), (Atsawasuwan et al., 2008; Csiszar, 2001; Decitre et al., 1998; Szauter et al., 2005). TGFβ in turn regulates the expression of many ECM proteins and modifying enzymes including LOXs, and TGFβ increases levels of factors that evoke inflammation, induce fibrosis and promote metastasis (Bierie and Moses, 2006; Oleggini et al., 2007). Indeed, force itself modulates TGFβ activation and compression alters growth factor signaling (Tschumperlin et al., 2004; Wipff et al., 2007). These findings underscore the dynamic and reciprocal relationship between ECM deposition, processing and degradation. Thus, cancer is best viewed as a dynamic, phenotypically-plastic and highly coordinated tissue remodeling process that is tightly regulated by biochemical and mechanical cues. Accordingly, not only will we need to clarify the role of ECM cleavage in tumors but we will also be obliged to understand how ECM remodeling is integrated within the context of its deposition, post translational modifications and topological rearrangement and to take into consideration the effect of mechanical force as a key regulator of malignancy.

Materials and Methods

Antibodies and Reagents

Antibodies were: β4 integrin (3E1); β1 integrin (AIIB2; Chemicon); FAK (77), YES (1), β1 integrin (18), E-Cadherin (610405; BD Transduction); laminin-5 (BM165; MP Marinkovich); β actin (AC-15; Sigma); ErbB2 (3B5; Calbiochem); polyclonal β catenin (Sigma); FAK^{pY397} (BioSource); Phospho-(Ser/Thr) Akt Substrates and Akt^{pS473}(Cell Signalling); Akt (BD Pharmingen); p130Cas, $ErbB2^{pY1248}$ (Abcam); cytokeratin 14 (Covance); LOX (A. Giaccia, Stanford University); LOX polyclonal activity inhibitory antibody (OpenBiosystems); and secondary AlexaFluor goat anti-mouse, anti-rabbit, and anti-rat (488- and 555 conjugates), AlexaFluor phalloidin (488-conjugate, Invitrogen); Donkey anti-mouse and anti-rabbit (Cy2- and Cy3-conjugates; Jackson ImmunoResearch); and Sheep anti-mouse and anti-rabbit HRP-linked (Amersham). Reagents included: LY294002; (50μm in DMSO; Calbiochem).

Cell manipulations

MEC and fibroblast cell lines were cultured as described (Paszek et al., 2005). Collagen crosslinking was induced by addition of 15mM L-ribose to the culture medium (Girton et al., 1999). rBM-conjugated PA gels with calibrated stiffness were prepared as described (Johnson et al., 2007).

Vector Constructs and gene expression

Full length human ErbB2 (K. Ignatoski) was cloned into the pRet puro Tet IRES EGFP tetracycline-inducible vector. The β1 integrin wild type, β1 integrin glycan wedge constitutively active and β1 integrin clustering mutant V737N constructs and the preparation of virus and cell infection and selection have been described (Paszek et al., 2005). Four myc-tags were added to the C-terminus of full length LOX and cloned into the pLV puro $TetO_7$mCMV tetracycline-inducible lentiviral vector and expressed biscistronically with EGFP.

Elastic modulus measurements

Mammary glands and gels were assayed for materials properties by unconfined compression and rheometrical analysis (Paszek et al., 2005).

Mice and Treatments

FVB-TgN MMTV-Neu, NOD/SCID, and BalbC nu/nu mice (Jackson Laboratory) were maintained in accordance with University of Pennsylvania and University of California IACUC guidelines. For LOX inhibition studies animals were treated with BAPN (3mg/kg; Spectrum) in the drinking water (4-8 mice/group; 4 studies) or a LOX function-blocking polyclonal (3mg/kg; OpenBiosystems, D8746) injected intraperitoneally twice per week (3-4 mice/; 1 study). Mice were sacrificed at 7-71/2 months of age at which time tail vein blood was collected. Lesions were detected by palpation (~3mm diameter) and tumor volume was assessed using calipers. At sacrifice mammary glands were excised, imaged and mechanically tested or snap frozen or paraformaldehyde fixed.

Tumor grading

Tumor grading was performed blinded on H&E stained sections from untreated (n=14) or BAPN treated (n=13) #2-3 mammary glands. Premalignant lesions were defined as hyperplastic alveolar hyperplasia (HAN) or Mammary Intraepithelial Neoplasia (MIN)-like foci. Grade I lesion were well defined as homogenous carcinomas, Grade II contained areas with strong necrosis, stromal reaction and/or red blood cells outside of tumor blood vessels and Grade III also contained necrosis and nuclear pleiomorphy. Adjacent tissue was defined as mammary tissue surrounding a tumor that was cut away from the tumor prior to subsequent analysis. A small set of anti-LOX treated mice (n=4) was compared with their controls (n=3), and showed the same tendency to less progressed lesions as was observed in the BAPN treated animals.

Xenograft manipulations

NOD/SCID mice (n=24) were used for mammary fat pad transplantation studies (Kuperwasser et al., 2004). Briefly, the rudimentary inguinal epithelium was removed from three week old anesthetized female mice and 5×10^5 NIH 3T3 WT or LOX-expressing fibroblasts (2.5×10^5 were treated with 4Gy irradiation 24 hours prior to injection) were injected into the left and right mammary glands. Two weeks following fibroblast injection, 1×10^6 DCIS.com MCF10AT MEC 4 day old rBM-generated, proliferating organoids (16-20 cells/organoid) were suspended in Dulbeccos modified PBS and injected into the pre-conditioned fat pads. All

mice were sacrificed at 8 weeks of age (3 weeks following MEC injection and 5 weeks after fibroblast injection), lesion volume was assessed by caliper measurement, photographed *In Situ*, and dissected gland fragments were imaged and mechanically-tested or snap frozen, or fixed and paraffin embedded.

Subcutaneous studies

Proliferating rBM-generated organoids (16-20 cells/organoid) from each experimental condition were injected subcutaneously into the rear flanks of BalbC Nu/Nu mice (6-8 mice/group; $5\text{-}10\times10^6$) and tumor formation was monitored for three weeks and samples were assessed as above at study termination.

Collagen crosslinking

Mammary gland collagen was reduced with standardized NaB^3H_4, hydrolyzed with 6N HCl and subjected to amino acid and collagen crosslink analyses as described (Yamauchi and Shiiba, 2008). The reducible crosslinks, dehydro-dihydroxylysinonorleucine (deH-DHLNL) and deH-hydroxylysinonorleucine (deH-HLNL), their ketoamines, were identified as their reduced forms, i.e. DHLNL and HLNL. The crosslinks analyzed (reducible and nonreducible) were quantified as moles/mole of collagen based on the hydroxyproline value of 300 residues per collagen molecule. LOX activity was measured in cell supernatant and plasma as described (Erler et al., 2006).

Immunostaining and Imaging

Immunofluorescence and imaging of 3D cultures and tissues was as described (Paszek et al., 2005). Picrosirius red analysis was achieved using paraffin sections of mammary glands stained with 0.1% Picrosirius Red (Direct Red 80; Sigma) and counterstained with Weigert's Hematoxylin to reveal fibrillar collagen. Sections were serially imaged using an Olympus IX81 fluorescence microscope fitted with an analyzer (U-ANT) and polarizer (U-POT; Olympus) oriented parallel and orthogonal to each other and quantified using minimal thresholding. Two-photon second harmonics imaging was performed on a Prairie Technology Ultima System attached to an Olympus BX-51 with a water immersion objective and samples were quantified by calculating the linearity of multiple collagen fibrils (see Appendix for further details).

Immunoblot analysis

Cells were lysed in RIPA or Laemmli buffer and assayed by immunoblotting (Johnson et al., 2007).

Statistics

Statistical analysis was performed with GraphPad Prism using an unpaired student's t-test, two-way ANOVA, or Fisher's exact test.

Supplementary Material

Refer to Web version on PubMed Central for supplementary material.

Acknowledgments

We thank K. Ignatoski for the ErbB2 construct, MP Marinkovich for the BM165 antibody, P. Mrass for 2 photon microscopy guidance and R.G. Wells for mentoring of KRL. The work was supported by NIH grants R01-CA078731 to VMW, R01-CA057621 to Z. Werb, and T32HL00795404 to KRL, and grants DOD W81XWH-05-1-330, DOE A107165 and CIRM RS1-00449 to VMW.

References

Atsawasuwan P, Mochida Y, Katafuchi M, Kaku M, Fong KS, Csiszar K, Yamauchi M. Lysyl oxidase binds transforming growth factor-beta and regulates its signaling via amine oxidase activity. J Biol Chem 2008;283:34229–34240. [PubMed: 18835815]

Bierie B, Chung CH, Parker JS, Stover DG, Cheng N, Chytil A, Aakre M, Shyr Y, Moses HL. Abrogation of TGF-beta signaling enhances chemokine production and correlates with prognosis in human breast cancer. J Clin Invest 2009;119:1571–1582. [PubMed: 19451693]

Bierie B, Moses HL. Tumour microenvironment: TGFbeta: the molecular Jekyll and Hyde of cancer. Nat Rev Cancer 2006;6:506–520. [PubMed: 16794634]

Bondareva A, Downey CM, Ayres F, Liu W, Boyd SK, Hallgrimsson B, Jirik FR. The lysyl oxidase inhibitor, beta-aminopropionitrile, diminishes the metastatic colonization potential of circulating breast cancer cells. PLoS One 2009;4:e5620. [PubMed: 19440335]

Butcher DT, Alliston T, Weaver VM. A tense situation: forcing tumour progression. Nat Rev Cancer 2009;9:108–122. [PubMed: 19165226]

Cabodi S, Tinnirello A, Di Stefano P, Bisaro B, Ambrosino E, Castellano I, Sapino A, Arisio R, Cavallo F, Forni G, et al. p130Cas as a new regulator of mammary epithelial cell proliferation, survival, and HER2-neu oncogene-dependent breast tumorigenesis. Cancer Res 2006;66:4672–4680. [PubMed: 16651418]

Colpaert CG, Vermeulen PB, Fox SB, Harris AL, Dirix LY, Van Marck EA. The presence of a fibrotic focus in invasive breast carcinoma correlates with the expression of carbonic anhydrase IX and is a marker of hypoxia and poor prognosis. Breast Cancer Res Treat 2003;81:137–147. [PubMed: 14572156]

Coussens LM, Fingleton B, Matrisian LM. Matrix metalloproteinase inhibitors and cancer: trials and tribulations. Science 2002;295:2387–2392. [PubMed: 11923519]

Coussens LM, Raymond WW, Bergers G, Laig-Webster M, Behrendtsen O, Werb Z, Caughey GH, Hanahan D. Inflammatory mast cells up-regulate angiogenesis during squamous epithelial carcinogenesis. Genes Dev 1999;13:1382–1397. [PubMed: 10364156]

Csiszar K. Lysyl oxidases: a novel multifunctional amine oxidase family. Prog Nucleic Acid Res Mol Biol 2001;70:1–32. [PubMed: 11642359]

Decitre M, Gleyzal C, Raccurt M, Peyrol S, Aubert-Foucher E, Csiszar K, Sommer P. Lysyl oxidase-like protein localizes to sites of de novo fibrinogenesis in fibrosis and in the early stromal reaction of ductal breast carcinomas. Lab Invest 1998;78:143–151. [PubMed: 9484712]

Erler JT, Bennewith KL, Cox TR, Lang G, Bird D, Koong A, Le QT, Giaccia AJ. Hypoxia-induced lysyl oxidase is a critical mediator of bone marrow cell recruitment to form the premetastatic niche. Cancer Cell 2009;15:35–44. [PubMed: 19111879]

Erler JT, Bennewith KL, Nicolau M, Dornhofer N, Kong C, Le QT, Chi JT, Jeffrey SS, Giaccia AJ. Lysyl oxidase is essential for hypoxia-induced metastasis. Nature 2006;440:1222–1226. [PubMed: 16642001]

Erler JT, Giaccia AJ. Lysyl oxidase mediates hypoxic control of metastasis. Cancer Res 2006;66:10238–10241. [PubMed: 17079439]

Erler JT, Weaver VM. Three-dimensional context regulation of metastasis. Clin Exp Metastasis 2009;26:35–49. [PubMed: 18814043]

Georges PC, Hui JJ, Gombos Z, McCormick ME, Wang AY, Uemura M, Mick R, Janmey PA, Furth EE, Wells RG. Increased stiffness of the rat liver precedes matrix deposition: implications for fibrosis. Am J Physiol Gastrointest Liver Physiol 2007;293:G1147–1154. [PubMed: 17932231]

Girton TS, Oegema TR, Tranquillo RT. Exploiting glycation to stiffen and strengthen tissue equivalents for tissue engineering. J Biomed Mater Res 1999;46:87–92. [PubMed: 10357139]

Hasebe T, Tsuda H, Tsubono Y, Imoto S, Mukai K. Fibrotic focus in invasive ductal carcinoma of the breast: a histopathological prognostic parameter for tumor recurrence and tumor death within three years after the initial operation. Jpn J Cancer Res 1997;88:590–599. [PubMed: 9263537]

Hu M, Yao J, Carroll DK, Weremowicz S, Chen H, Carrasco D, Richardson A, Violette S, Nikolskaya T, Nikolsky Y, et al. Regulation of in situ to invasive breast carcinoma transition. Cancer Cell 2008;13:394–406. [PubMed: 18455123]

Jodele S, Blavier L, Yoon JM, DeClerck YA. Modifying the soil to affect the seed: role of stromal-derived matrix metalloproteinases in cancer progression. Cancer Metastasis Rev 2006;25:35–43. [PubMed: 16680570]

Johnson KR, Leight JL, Weaver VM. Demystifying the effects of a three-dimensional microenvironment in tissue morphogenesis. Methods Cell Biol 2007;83:547–583. [PubMed: 17613324]

Kagan HM, Li W. Lysyl oxidase: properties, specificity, and biological roles inside and outside of the cell. J Cell Biochem 2003;88:660–672. [PubMed: 12577300]

Katz M, Amit I, Citri A, Shay T, Carvalho S, Lavi S, Milanezi F, Lyass L, Amariglio N, Jacob-Hirsch J, et al. A reciprocal tensin-3-cten switch mediates EGF-driven mammary cell migration. Nat Cell Biol 2007;9:961–969. [PubMed: 17643115]

Kim H, Muller WJ. The role of the epidermal growth factor receptor family in mammary tumorigenesis and metastasis. Exp Cell Res 1999;253:78–87. [PubMed: 10579913]

Kirschmann DA, Seftor EA, Fong SF, Nieva DR, Sullivan CM, Edwards EM, Sommer P, Csiszar K, Hendrix MJ. A molecular role for lysyl oxidase in breast cancer invasion. Cancer Res 2002;62:4478–4483. [PubMed: 12154058]

Kolacna L, Bakesova J, Varga F, Kostakova E, Planka L, Necas A, Lukas D, Amler E, Pelouch V. Biochemical and biophysical aspects of collagen nanostructure in the extracellular matrix. Physiol Res 2007;56:S51–60. [PubMed: 17552894]

Koukoulis GK, Howeedy AA, Korhonen M, Virtanen I, Gould VE. Distribution of tenascin, cellular fibronectins and integrins in the normal, hyperplastic and neoplastic breast. J Submicrosc Cytol Pathol 1993;25:285–295. [PubMed: 7686813]

Kuperwasser C, Chavarria T, Wu M, Magrane G, Gray JW, Carey L, Richardson A, Weinberg RA. Reconstruction of functionally normal and malignant human breast tissues in mice. Proc Natl Acad Sci U S A 2004;101:4966–4971. [PubMed: 15051869]

Lahlou H, Sanguin-Gendreau V, Zuo D, Cardiff RD, McLean GW, Frame MC, Muller WJ. Mammary epithelial-specific disruption of the focal adhesion kinase blocks mammary tumor progression. Proc Natl Acad Sci U S A 2007;104:20302–20307. [PubMed: 18056629]

Lo CM, Wang HB, Dembo M, Wang YL. Cell movement is guided by the rigidity of the substrate. Biophys J 2000;79:144–152. [PubMed: 10866943]

Lucero HA, Kagan HM. Lysyl oxidase: an oxidative enzyme and effector of cell function. Cell Mol Life Sci. 2006

Madan R, Smolkin MB, Cocker R, Fayyad R, Oktay MH. Focal adhesion proteins as markers of malignant transformation and prognostic indicators in breast carcinoma. Hum Pathol 2006;37:9–15. [PubMed: 16360410]

Martin LJ, Boyd NF. Mammographic density. Potential mechanisms of breast cancer risk associated with mammographic density: hypotheses based on epidemiological evidence. Breast Cancer Res 2008;10:201. [PubMed: 18226174]

Martin MD, Carter KJ, Jean-Philippe SR, Chang M, Mobashery S, Thiolloy S, Lynch CC, Matrisian LM, Fingleton B. Effect of ablation or inhibition of stromal matrix metalloproteinase-9 on lung metastasis in a breast cancer model is dependent on genetic background. Cancer Res 2008;68:6251–6259. [PubMed: 18676849]

Miranti CK, Brugge JS. Sensing the environment: a historical perspective on integrin signal transduction. Nat Cell Biol 2002;4:E83–90. [PubMed: 11944041]

Mitra SK, Schlaepfer DD. Integrin-regulated FAK-Src signaling in normal and cancer cells. Curr Opin Cell Biol 2006;18:516–523. [PubMed: 16919435]

Muthuswamy SK, Li D, Lelievre S, Bissell MJ, Brugge JS. ErbB2, but not ErbB1, reinitiates proliferation and induces luminal repopulation in epithelial acini. Nat Cell Biol 2001;3:785–792. [PubMed: 11533657]

Oleggini R, Gastaldo N, Di Donato A. Regulation of elastin promoter by lysyl oxidase and growth factors: cross control of lysyl oxidase on TGF-beta1 effects. Matrix Biol 2007;26:494–505. [PubMed: 17395448]

Page-McCaw A, Ewald AJ, Werb Z. Matrix metalloproteinases and the regulation of tissue remodelling. Nat Rev Mol Cell Biol 2007;8:221–233. [PubMed: 17318226]

Paszek MJ, Zahir N, Johnson KR, Lakins JN, Rozenberg GI, Gefen A, Reinhart-King CA, Margulies SS, Dembo M, Boettiger D, et al. Tensional homeostasis and the malignant phenotype. Cancer Cell 2005;8:241–254. [PubMed: 16169468]

Payne SL, Hendrix MJ, Kirschmann DA. Paradoxical roles for lysyl oxidases in cancer--a prospect. J Cell Biochem 2007;101:1338–1354. [PubMed: 17471532]

Pfeiffer BJ, Franklin CL, Hsieh FH, Bank RA, Phillips CL. Alpha 2(I) collagen deficient oim mice have altered biomechanical integrity, collagen content, and collagen crosslinking of their thoracic aorta. Matrix Biol 2005;24:451–458. [PubMed: 16095890]

Postovit LM, Abbott DE, Payne SL, Wheaton WW, Margaryan NV, Sullivan R, Jansen MK, Csiszar K, Hendrix MJ, Kirschmann DA. Hypoxia/reoxygenation: a dynamic regulator of lysyl oxidase-facilitated breast cancer migration. J Cell Biochem 2008;103:1369–1378. [PubMed: 17685448]

Ramaswamy S, Ross KN, Lander ES, Golub TR. A molecular signature of metastasis in primary solid tumors. Nat Genet 2003;33:49–54. [PubMed: 12469122]

Sawada Y, Tamada M, Dubin-Thaler BJ, Cherniavskaya O, Sakai R, Tanaka S, Sheetz MP. Force sensing by mechanical extension of the Src family kinase substrate p130Cas. Cell 2006;127:1015–1026. [PubMed: 17129785]

Sinkus R, Lorenzen J, Schrader D, Lorenzen M, Dargatz M, Holz D. High-resolution tensor MR elastography for breast tumour detection. Phys Med Biol 2000;45:1649–1664. [PubMed: 10870716]

Sternlicht MD, Lochter A, Sympson CJ, Huey B, Rougier JP, Gray JW, Pinkel D, Bissell MJ, Werb Z. The stromal proteinase MMP3/stromelysin-1 promotes mammary carcinogenesis. Cell 1999;98:137–146. [PubMed: 10428026]

Szauter KM, Cao T, Boyd CD, Csiszar K. Lysyl oxidase in development, aging and pathologies of the skin. Pathol Biol (Paris) 2005;53:448–456. [PubMed: 16085123]

Tetu B, Brisson J, Wang CS, Lapointe H, Beaudry G, Blanchette C, Trudel D. The influence of MMP-14, TIMP-2 and MMP-2 expression on breast cancer prognosis. Breast Cancer Res 2006;8:R28. [PubMed: 16776850]

Tschumperlin DJ, Dai G, Maly IV, Kikuchi T, Laiho LH, McVittie AK, Haley KJ, Lilly CM, So PT, Lauffenburger DA, et al. Mechanotransduction through growth-factor shedding into the extracellular space. Nature 2004;429:83–86. [PubMed: 15103386]

van der Slot AJ, van Dura EA, de Wit EC, De Groot J, Huizinga TW, Bank RA, Zuurmond AM. Elevated formation of pyridinoline cross-links by profibrotic cytokines is associated with enhanced lysyl hydroxylase 2b levels. Biochim Biophys Acta 2005;1741:95–102. [PubMed: 15955452]

Webster MA, Hutchinson JN, Rauh MJ, Muthuswamy SK, Anton M, Tortorice CG, Cardiff RD, Graham FL, Hassell JA, Muller WJ. Requirement for both Shc and phosphatidylinositol 3′ kinase signaling pathways in polyomavirus middle T-mediated mammary tumorigenesis. Mol Cell Biol 1998;18:2344–2359. [PubMed: 9528804]

White DE, Kurpios NA, Zuo D, Hassell JA, Blaess S, Mueller U, Muller WJ. Targeted disruption of beta1-integrin in a transgenic mouse model of human breast cancer reveals an essential role in mammary tumor induction. Cancer Cell 2004;6:159–170. [PubMed: 15324699]

Wipff PJ, Rifkin DB, Meister JJ, Hinz B. Myofibroblast contraction activates latent TGF-beta1 from the extracellular matrix. J Cell Biol 2007;179:1311–1323. [PubMed: 18086923]

Wolf K, Wu YI, Liu Y, Geiger J, Tam E, Overall C, Stack MS, Friedl P. Multi-step pericellular proteolysis controls the transition from individual to collective cancer cell invasion. Nat Cell Biol 2007;9:893–904. [PubMed: 17618273]

Yamauchi M, Shiiba M. Lysine hydroxylation and cross-linking of collagen. Methods Mol Biol 2008;446:95–108. [PubMed: 18373252]

Zaman MH, Trapani LM, Sieminski AL, Mackellar D, Gong H, Kamm RD, Wells A, Lauffenburger DA, Matsudaira P. Migration of tumor cells in 3D matrices is governed by matrix stiffness along with cell-matrix adhesion and proteolysis. Proc Natl Acad Sci U S A 2006;103:10889–10894. [PubMed: 16832052]

Zhang B, Cao X, Liu Y, Cao W, Zhang F, Zhang S, Li H, Ning L, Fu L, Niu Y, et al. Tumor-derived matrix metalloproteinase-13 (MMP-13) correlates with poor prognoses of invasive breast cancer. BMC Cancer 2008;8:83. [PubMed: 18373849]

Zhao Y, Min C, Vora S, Trackman PC, Sonenshein GE, Kirsch KH. The lysyl oxidase pro-peptide attenuates fibronectin-mediated activation of FAK and p130CAS in breast cancer cells. J Biol Chem. 2008

Zutter MM, Sun H, Santoro SA. Altered integrin expression and the malignant phenotype: the contribution of multiple integrated integrin receptors. J Mammary Gland Biol Neoplasia 1998;3:191–200. [PubMed: 10819527]

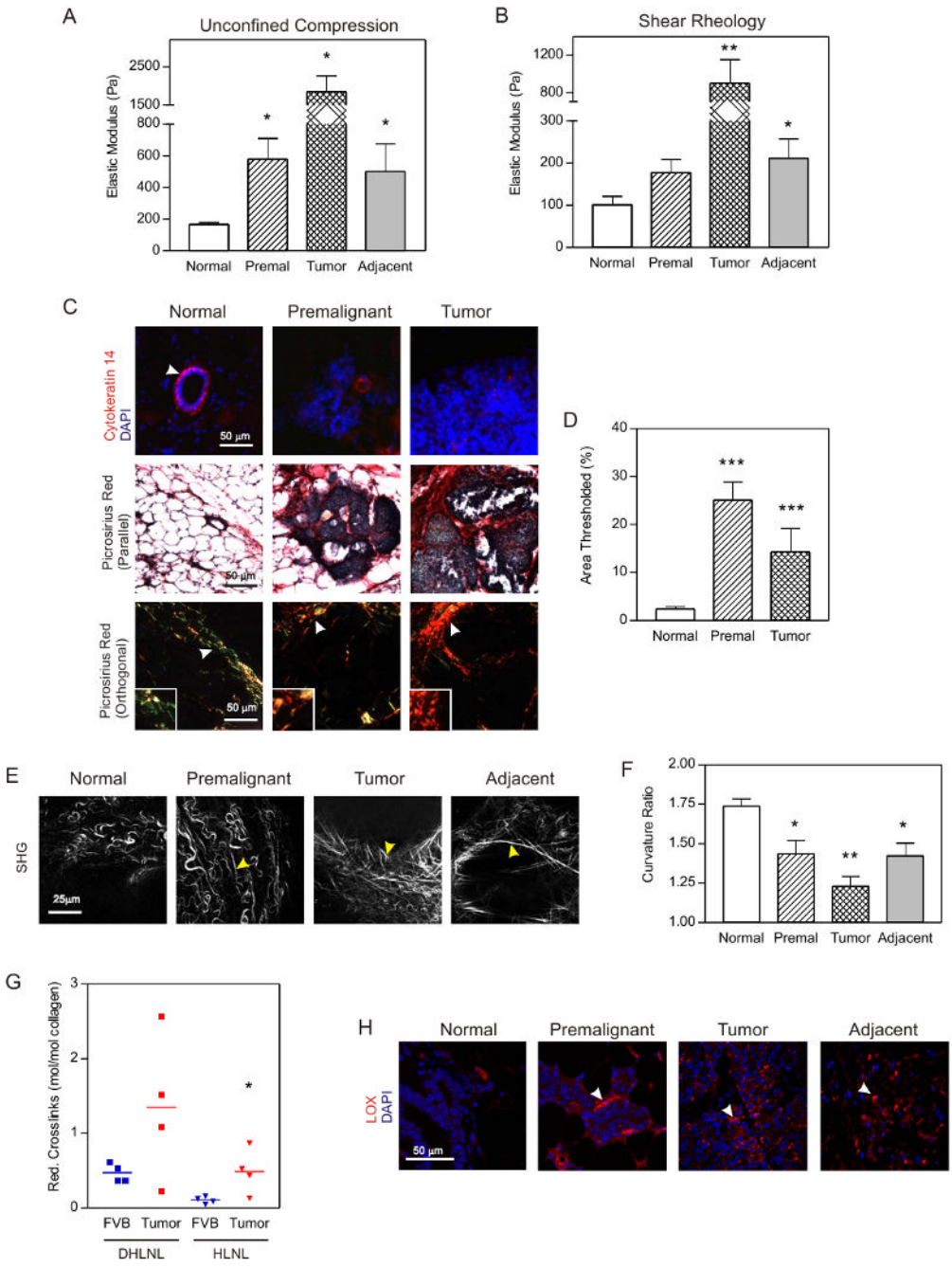

Figure 1. ECM stiffening, collagen crosslinking and tissue fibrosis accompany breast transformation

A. Elastic modulus of mammary glands from FVB MMTV-Neu mice at different stages of tumor progression measured by unconfined compression. **B.** Shear rheology of tissues described in A. **C.** Top row: Confocal images of tissues in A stained for cytokeratin 14 (red) and DAPI (nuclei; blue). Middle and bottom rows: Photomicrographs of tissues in A stained with Picrosirius Red and hematoxylin, viewed under parallel (middle), and orthogonal polarizing filters (bottom). **D.** Quantification of images in C. **E.** SHG images of tissues described in A. **F.** Quantification of images in E. **G.** Scatter plot of collagen crosslinks. **H.** Confocal images of tissues described in A. stained for lysyl oxidase (LOX; red) and DAPI

(nuclei; blue). Images 40×, Bar 50μm. Values in A, B & D; Mean ± SEM of 4-6 glands/condition. * $p \leq 0.05$, ** $p \leq 0.01$, *** $p \leq 0.001$.

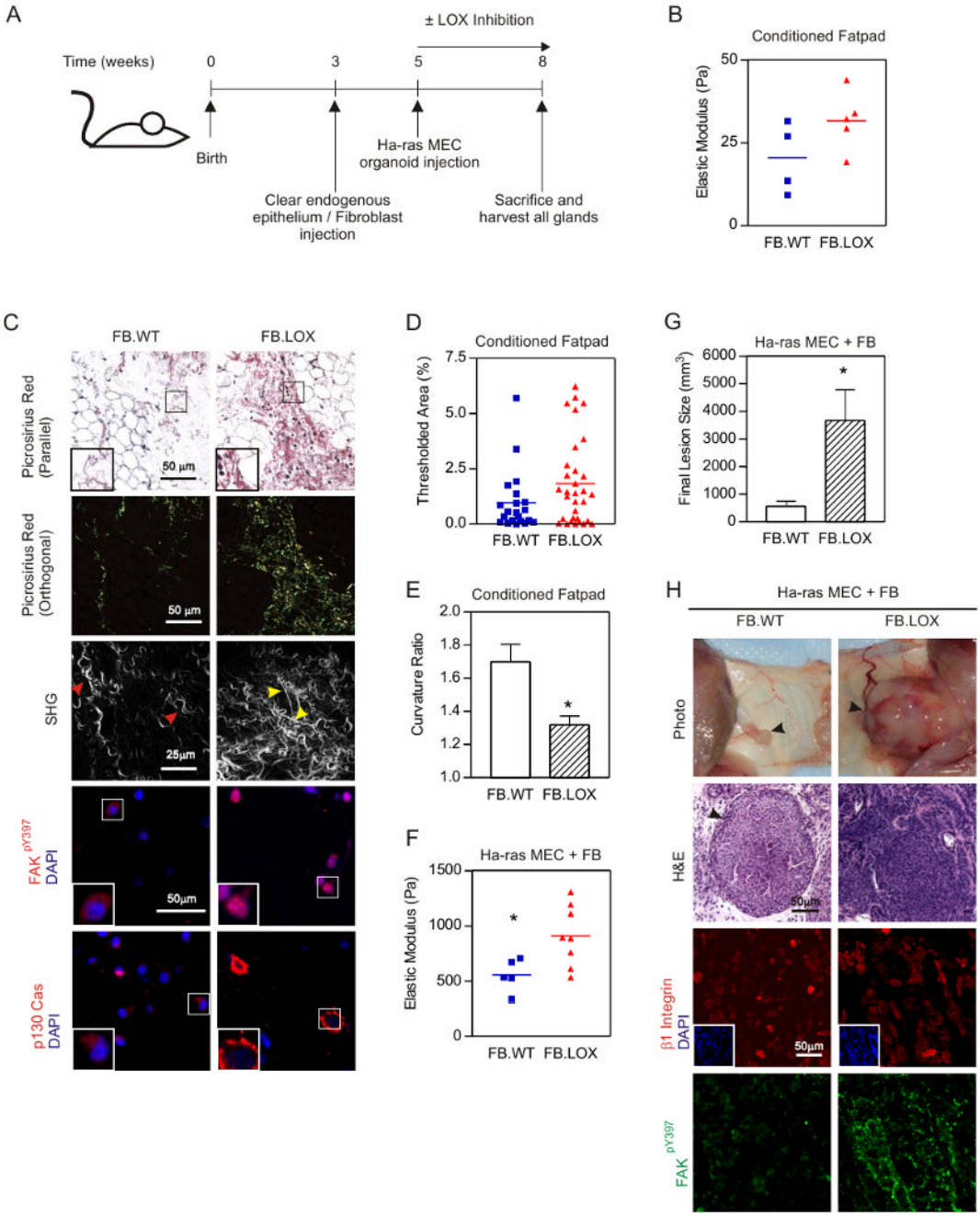

Figure 2. Collagen remodeling and tissue stiffening promote focal adhesions and tumor invasion

A. Experimental design. **B.** Scatter plot of breast rheology following LOX (FB.LOX) or control (FB.ctrl) fibroblast conditioning. **C.** Top two panels: Photomicrographs of tissues described in B stained with Picrosirius Red and hematoxylin viewed under parallel and orthogonal polarizing filters. Bar 50μm. Third panel: SHG images of tissues from fibroblast-conditioned mammary glands. Bar 25μm. Fourth and fifth panels: Confocal images of fibroblasts residing within fibroblast-conditioned mammary glands stained for active FAK (FAK^{pY397}; red; fourth panel), ^{p130}Cas (red; fifth panel) and DAPI (nuclei; blue). Bar 50μm. **D.** Scatter plot of fibrillar collagen in tissue shown in C. **E.** Scatter plot of collagen linearity measured by Curvature Ratio from SHG images shown in C. **F.** Rheology of mammary glands with injected Ha-ras

MCF10AT MECs. **G.** Lesion burden for mouse cohorts. **H.** Top: Photographs of mammary glands three weeks after injection with Ha-ras MCF10AT organoids. Middle: H&E stained tissue of MECs from lesions shown in H. Bottom: Confocal images of MECs in tissue shown in H stained for β1 integrin (red), active FAK (FAK^{pY397}; green) and DAPI (nuclei; blue; insert). Bar 50μm. Values in E and G are Mean ± SEM of several glands. * $p \leq 0.05$.

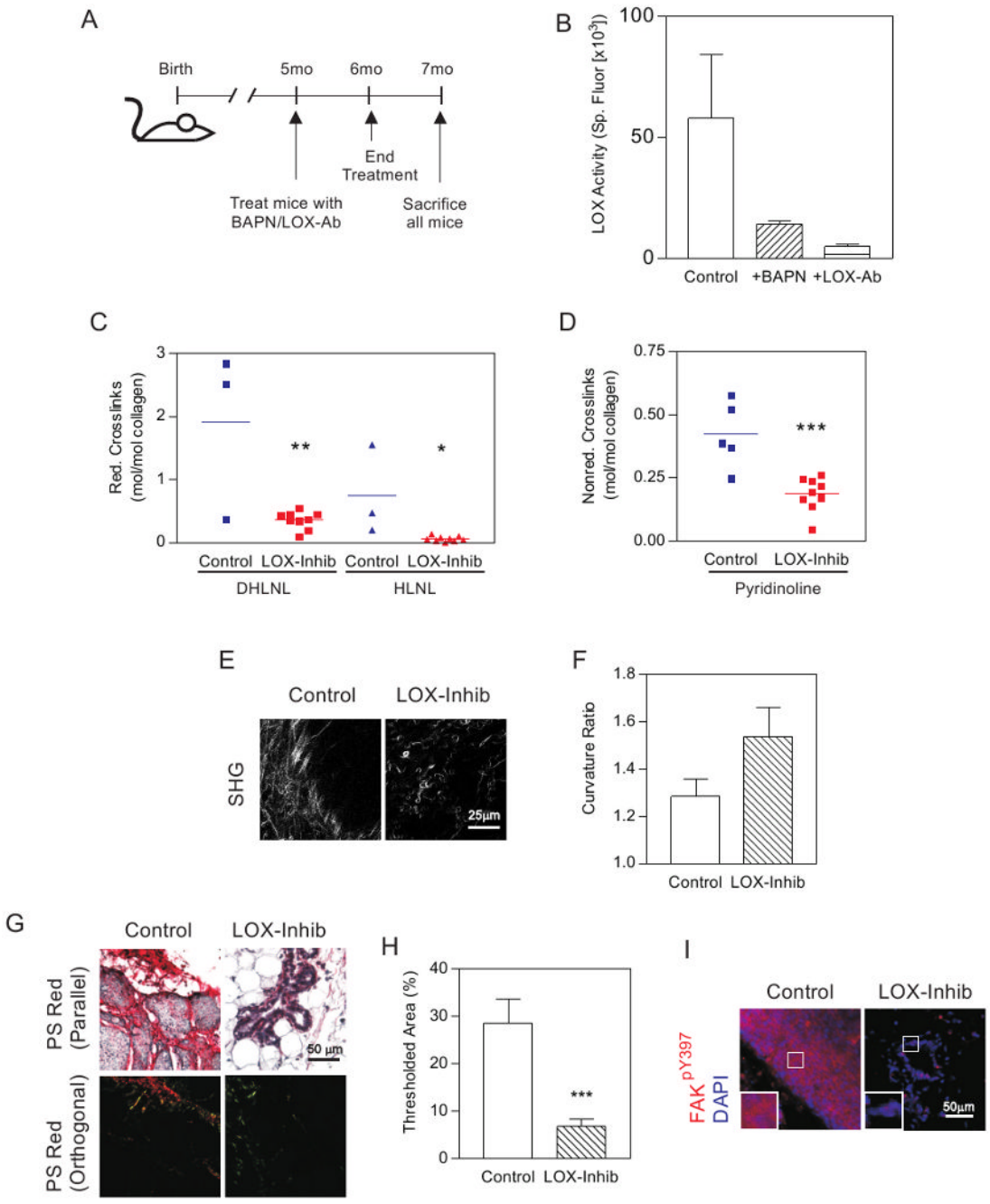

Figure 3. Inhibiting collagen crosslinking tempers tissue fibrosis and reduces focal adhesions

A. Experimental design. **B.** LOX enzymatic activity in serum of untreated (Control) compared to BAPN (+BAPN) or LOX inhibitory antibody-treated (+LOX-Ab) Neu mice. Values: Mean ± SEM. **C.** Scatter plots of reducible collagen crosslinks in LOX-inhibited (LOX-Inhib) and untreated (Control) Neu breasts. **D.** Scatter plots of pyridinoline in LOX-inhibited (LOX-Inhib) and untreated (Control) Neu breasts. **E.** SHG images of mammary glands from BAPN treated animals as described above. Bar 25μm. **F.** Collagen curvature in SHG images from D. (Supp Methods). Mean ± SEM 3-5 regions/4 glands/condition. **G.** Photomicrographs of sections from control and BAPN treated (LOX-Inhib) Neu mammary glands stained with Picrosirius Red and hematoxylin viewed under parallel or orthogonal polarizing filters. Bar 50μm. **H.** Fibrillar

collagen in control and LOX inhibited glands from images shown in F. Mean ± SEM of 4-6 images/4-8 glands/condition. **I.** Confocal images of sections from control and BAPN treated Neu glands stained for active FAK (FAK^{pY397}; red) and DAPI (nuclei; blue). Bar 50μm.* $p \leq 0.05$, ** $p \leq 0.01$, *** $p \leq 0.001$.

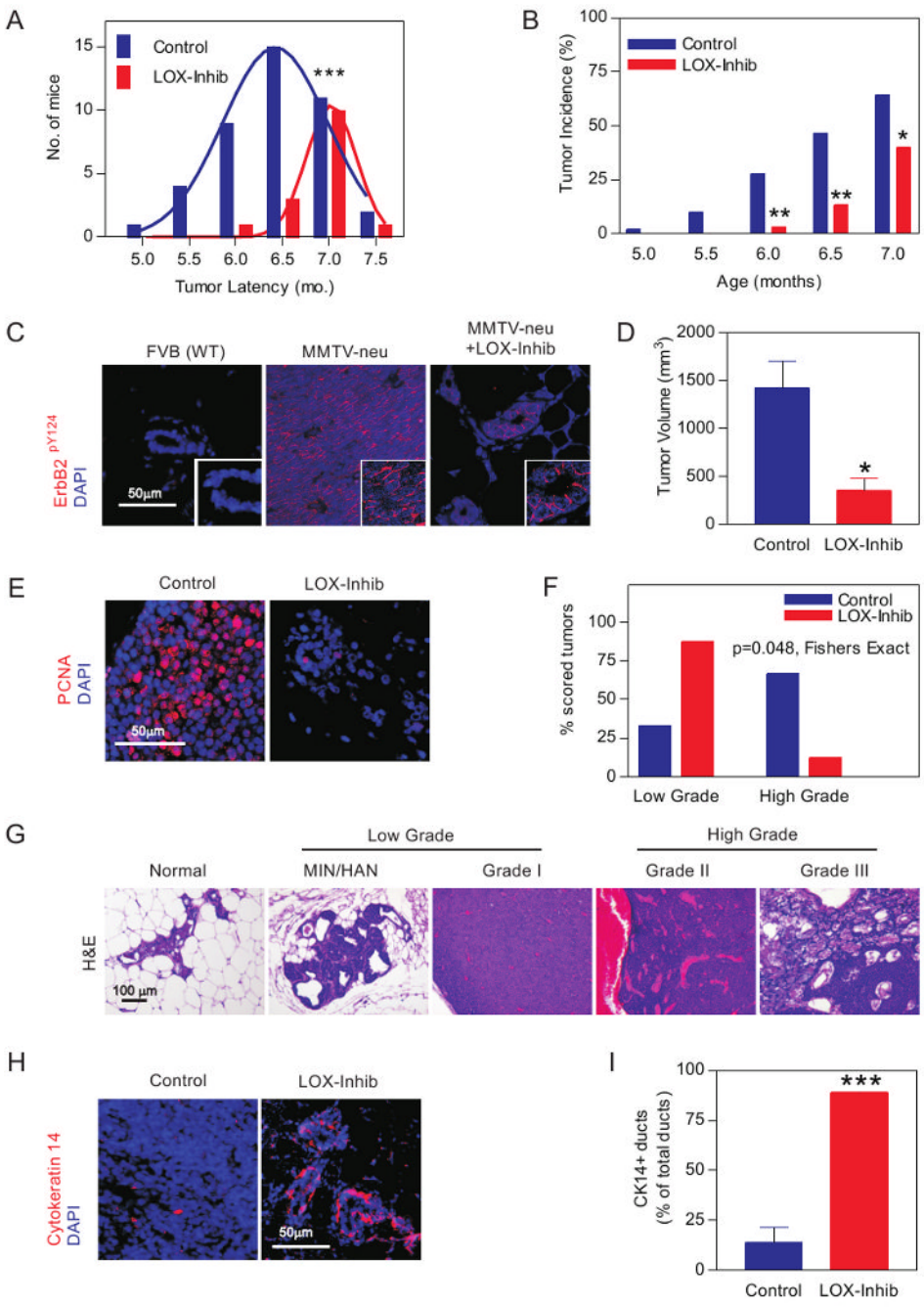

Figure 4. Inhibiting crosslinking reduces tissue fibrosis and tumor incidence and enhances tumor latency

A. Tumor latency. **B.** Tumor incidence without (Control) or with LOX inhibition (LOX-Inhib). **C.** Confocal images of activate ErbB2 (ErbB2^{pY1248}; red) in tissues from FVB non transgenic littermates, Neu (MMTV-Neu) and LOX inhibited mice (MMTV-Neu +LOX-Inhib). Bar 50μm. **D.** Tumor size in control and LOX inhibited mice. **E.** Confocal images of sections from LOX inhibited and control glands stained for PCNA (red) and DAPI (nuclei; blue). Bar 50μm. **F.** Grading of tumor lesions from mammary glands of control (n=14) and BAPN treated (LOX-Inhib, n=13) animals. **H.** H&E stained tissue showing typical Normal Glandular structure, Hyperplastic alveolar nodules (HAN) and mammary intraepithelial neoplasia (MIN)

premalignant lesions and Grades I, II and III ductal tumors. **I.** Confocal images of breast tissue stained for cytokeratin 14 (red) and DAPI (nuclei; blue) in control and LOX inhibited tissue. Bar 50μm. **I.** Percent cytokeratin 14 positive glands detected in breast from control and LOX inhibited animals. Values in A, B, D, F & I; Mean ± SEM of 4-6 measurements/4-12 tissue sections/group. * $p \leq 0.05$, ** $p \leq 0.01$, *** $p \leq 0.001$.

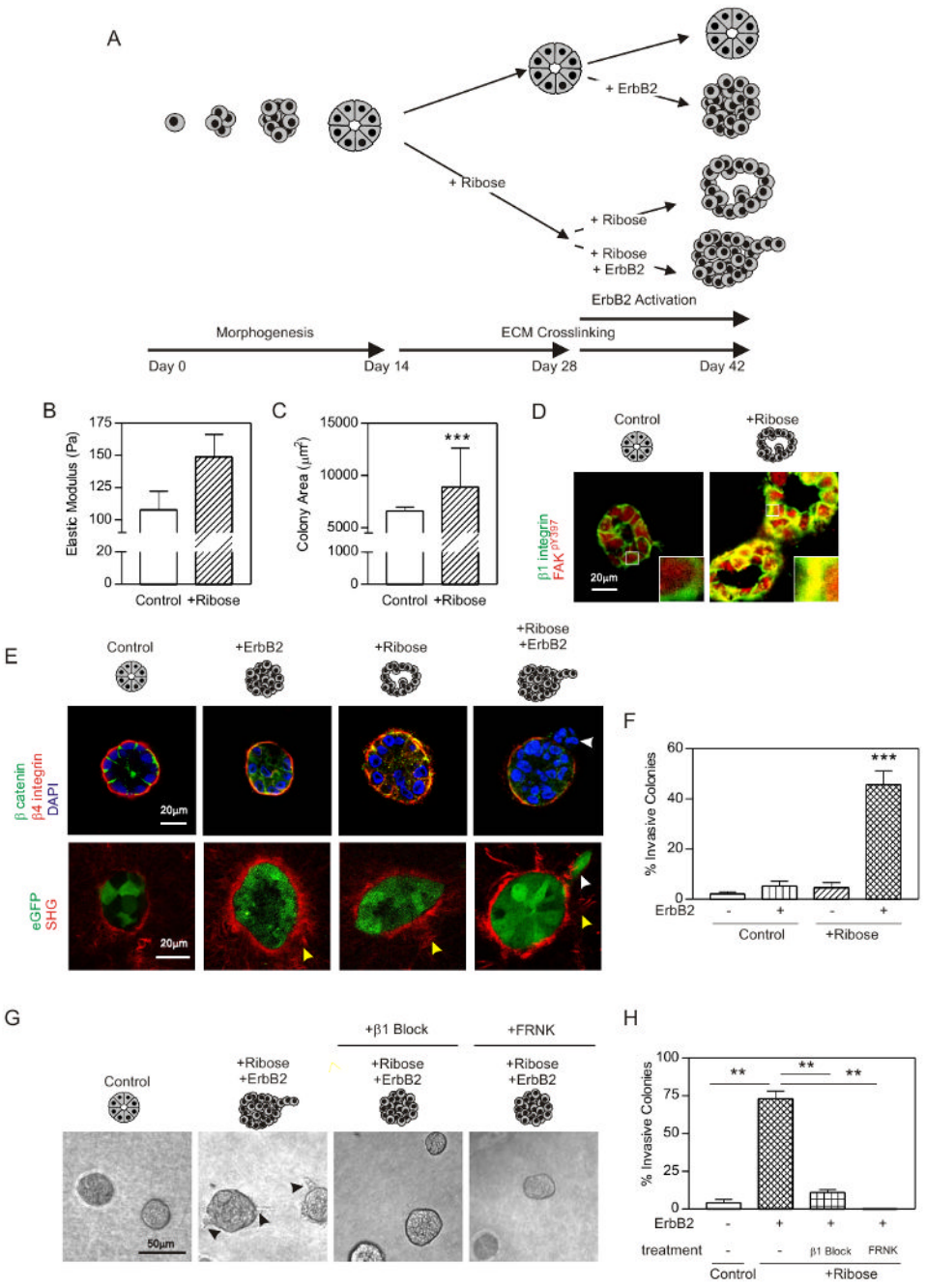

Figure 5. Collagen crosslinking and ECM stiffening promote focal adhesions and invasion of ErbB2 mammary colonies

A. Experimental design. **B.** Elastic modulus of ribose crosslinked (+Ribose) and untreated (Control) collagen gels. **C.** Cross sectional area of MEC colonies in +Ribose and Control gels. **D.** Confocal images of MCF10A colonies stained for β1 integrin (green), activate FAK (FAK^{pY397}; red) and DAPI (nuclei; blue) in Control and +Ribose gels. Bar 20μm. **E.** Top panels: Confocal images of MEC colonies expressing the ErbB2 chimera stained for β catenin (green), β4 integrin (red) and DAPI (nuclei; blue) in Control or +Ribose gels with (+ErbB2) or without ErbB2 activity. Bottom panels: SHG images of collagen fibrils and confocal images of eGFP expressing MEC colonies as described above. Bar 20μm. Yellow arrows identify

collagen bundles surrounding the colony periphery and white arrows indicate an invading MEC. **F.** Percent colony invasion shown in E. **G.** Phase contrast images of MEC colonies expressing the ErbB2 chimera in Control or +Ribose gels, with active ErbB2 (+ErbB2); co expressing a doxycycline inducible FRNK (right panel) or treated with β1 integrin function blocking antibody (+β1 block). **H.** Percent colony invasion shown in G. Values in B, C, F & H; Mean ± SEM from 3-5 experiments and/or 50-100 colonies in 3 experiments. ** $p \leq 0.01$, *** $p \leq 0.001$.

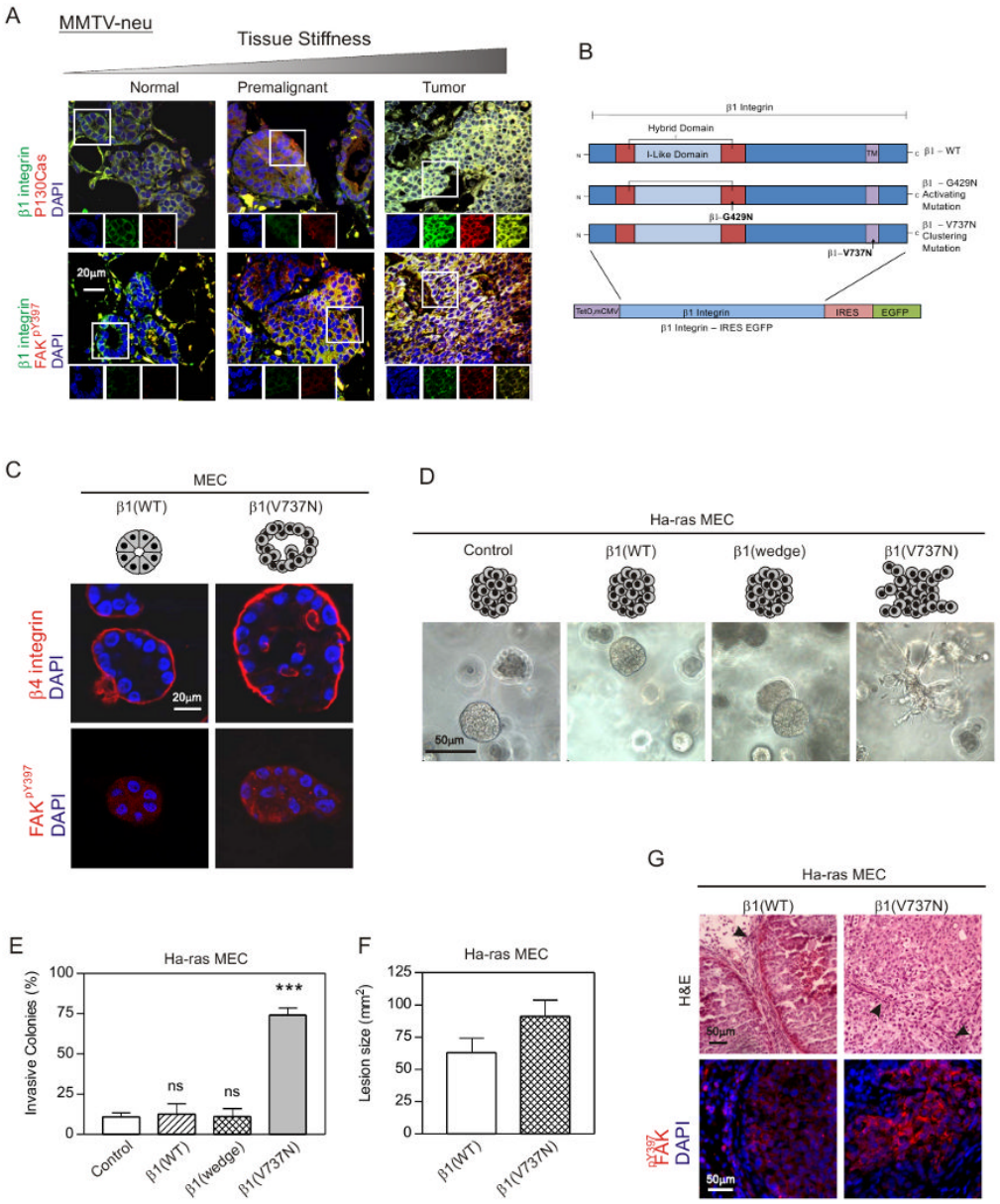

Figure 6. β1 integrin clustering promotes focal adhesions and drives invasion of a premalignant mammary epithelium in culture and *in vivo*

A. Combined and split (inserts) confocal images of tissue sections from MMTV-Neu breast stained for DAPI (nuclei; blue) and p130Cas (red; top), or β1 integrin (green; bottom) and, activate FAK (FAK^{pY397}; red). Bar 20μm. (colocalization analysis of the malignant tumors: FAK^{pY397} and β1 integrin, Pearson's r = 0.78; ^{p130}Cas and β1 integrin, Pearson's r = 0.89) **B.** β1 integrin constructs used for the studies shown in C-G. **C.** Confocal images of MCF10A MEC rBM colonies expressing the β1 integrin wild type (β1(WT)) or clustering mutant (β1 (V737N)) stained for β4 integrin (red; top), active FAK (FAK^{pY397}; red; bottom) and DAPI (nuclei; blue). **D.** Phase contrast images of Ha-ras MCF10AT MEC colonies expressing the β1 integrin wild type, glycan wedge or integrin cluster mutant in rBM. Bar 50μm. **E.** Percent invasion of the colonies shown in D **F.** Lesion size formed by Ha-ras MCF10AT MECs expressing the clustering β1 integrin mutation (β1(V737N)) and wild type integrin (β1(WT)).

G. Top panels: Photomicrographs of H&E stained sections of tumors formed by Ha-ras MECs expressing the clustering β1 integrin mutation (β1(V737N)) and wild type integrin (β1(WT)). Bottom panels: Confocal images of tissues stained for active FAK (FAK^{pY397}; red) and DAPI (nuclei; blue). Bar 50μm. Values in E & F; Mean ± SEM; 12-50 measurements/3 experiments *** $p \leq 0.001$.

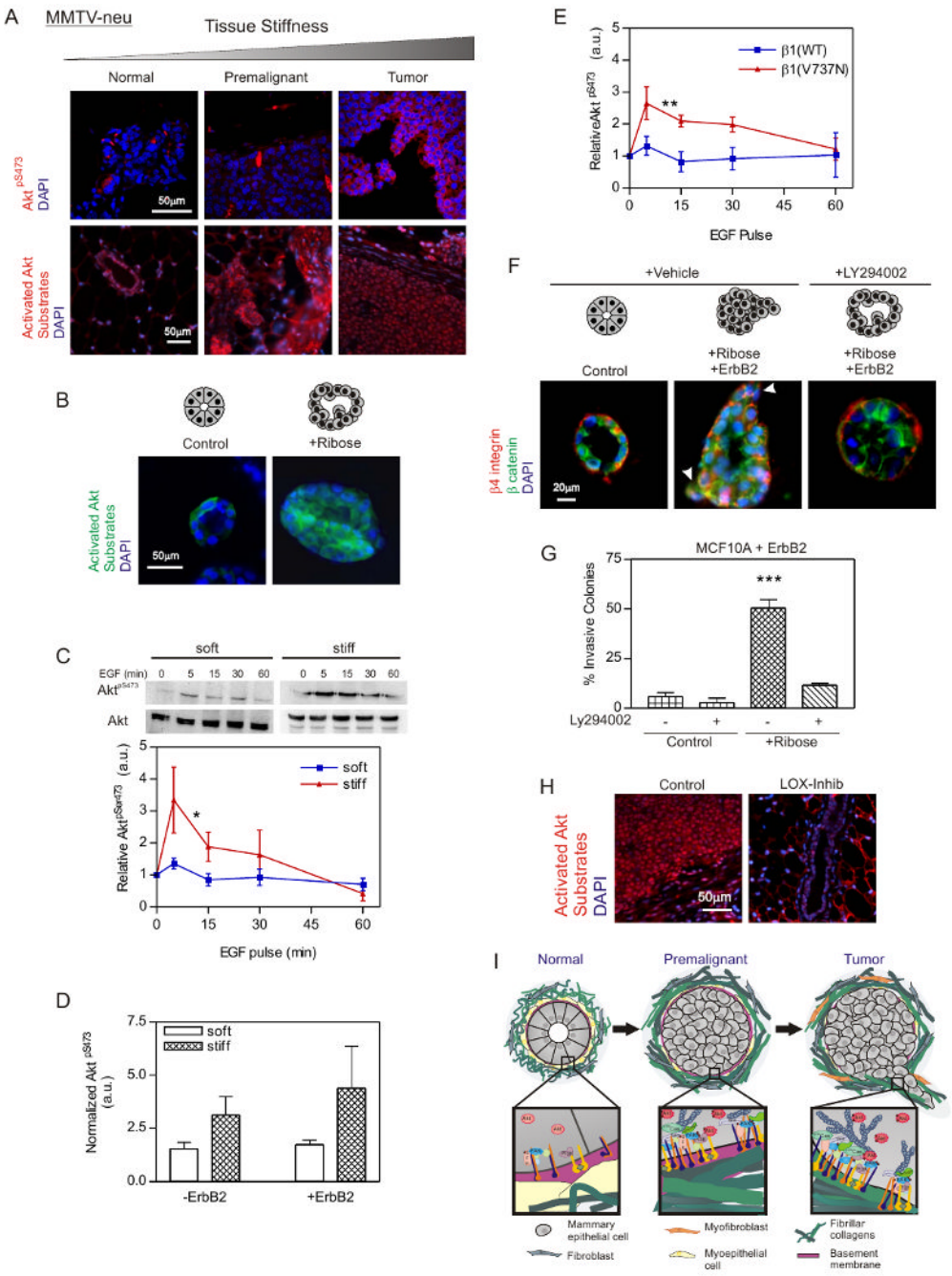

Figure 7. Tissue stiffness promotes integrin clustering and enhances growth factor-dependent PI3K activation

A. Confocal images of tissue from MMTV-Neu breast stained for Activated Akt^{pS473} (red; top panels), active Akt Substrate (red; bottom panels) and DAPI (nuclei; blue). Bar 50μm. **B.** Confocal images of MEC colonies in untreated (Control) or ribose-crosslinked (+Ribose) collagen/rBM gels stained for active Akt substrate (green) and DAPI (nuclei; blue). Bar 50μm. **C.** Immunoblots and line graph of time course of Akt^{pS473} and total Akt in EGF treated MCF10A MECs on soft and stiff rBM-PA gels. **D.** Ratio of Akt^{pS473} to total Akt in MCF10A MECS with active (+ErbB2; Dox induced) and nonactive wild type ErbB2 (-ErbB2: non-induced) on soft and stiff rBM-PA gels. **E.** Time course of EGF activated Akt^{pS473} to total Akt

in MCF10A MECs expressing the wild type β1 integrin (β1(WT)) or the β1 integrin cluster mutant (β1(V737N)) on soft rBM-PA gels. **F.** Confocal images of MCF10A MEC colonies stained for β catenin (green), β4 integrin (red) and DAPI (nuclei; blue) in control or ribose-crosslinked collagen/rBM gels in the presence (+ErbB2) or absence of doxycycline; with or without the PI3K inhibitor, LY294002. Bar 20μm. **G.** Quantification of invasive colonies from F. **H.** Confocal images of sections from control and LOX inhibited Neu mice stained for active Akt substrate (red) and DAPI (nuclei, blue). Bar 50μm. **I.** Cartoon showing effect of ECM stiffness on mammary colony behavior. Values in C, D and E; Mean ± SEM of 3 experiments, 50-100 colonies/experiment. * $p \leq 0.05$, ** $p \leq 0.01$, *** $p \leq 0.001$.